# *Anabaena* Flavodoxin as an Electron Carrier from Photosystem I to Ferredoxin-NADP$^+$ Reductase. Role of Flavodoxin Residues in Protein−Protein Interaction and Electron Transfer†

Isabel Nogués,‡ Manuel Hervás,§ José R. Peregrina,‡ José A. Navarro,§ Miguel A. de la Rosa,§ Carlos Gómez-Moreno,‡ and Milagros Medina*,‡

*Departamento de Bioquímica y Biología Molecular y Celular, Facultad de Ciencias, and Institute of Biocomputation and Physics of Complex Systems (BIFI), Facultad de Ciencias, Universidad de Zaragoza, 50009 Zaragoza, Spain, and Instituto de Bioquímica Vegetal y Fotosíntesis, Universidad de Sevilla-CSIC, CIC Isla de la Cartuja, Américo Vespucio 49, 41092 Sevilla, Spain*

*Received August 5, 2004; Revised Manuscript Received October 20, 2004*

ABSTRACT: Biochemical and structural studies indicate that electrostatic and hydrophobic interactions are critical in the formation of optimal complexes for efficient electron transfer (ET) between ferredoxin-NADP$^+$ reductase (FNR) and ferredoxin (Fd). Moreover, it has been shown that several charged and hydrophobic residues on the FNR surface are also critical for the interaction with flavodoxin (Fld), although, so far, no key residue on the Fld surface has been found to be the counterpart of such FNR side chains. In this study, negatively charged side chains on the Fld surface have been individually modified, either by the introduction of positive charges or by their neutralization. Our results indicate that although Glu16, Glu20, Glu61, Asp65, and Asp96 contribute to the orientation and optimization of the Fld interaction, either with FNR or with photosystem I (PSI) (presumably through the formation of salt bridges), for efficient ET, none of these side chains is involved in the formation of crucial salt bridges for optimal interaction with FNR. These data support the idea that the FNR−Fld interaction is less specific than the FNR−Fd interaction. However, analysis of the reactivity of these mutated Flds toward the membrane-anchored PSI complex indicated that all mutants, except Glu16Gln, lack the ability to form a stable complex with PSI. Thr12, Thr56, Asn58, and Asn97 are present in the close environment of the isoalloxazine ring of FMN in *Anabaena* Fld. Their roles in the interaction with and ET to FNR and PSI have also been studied. Mutants at these Fld positions indicate that residues in the close environment of the isoalloxazine ring modulate the ability of Fld to bind to and to exchange electrons with its physiological counterparts.

Electrostatic and hydrophobic interactions play an important role in the formation of optimal complexes for efficient electron transfer (ET)[1] between proteins (*1*, *2*). In the photosynthetic ET chain, electrons are transferred from photosystem I (PSI) to ferredoxin-NADP$^+$ reductase (FNR) via ferredoxin (Fd). In this system, specific recognition and binding between FNR and Fd are required for efficient ET (*3*−*7*). Thus, electrostatic interactions orient the proteins for formation of an initial complex, whereas hydrophobic interactions are critical in the formation of the optimal complex for ET (*5*, *6*, *8*). The structures of the FNR−Fd complexes from *Anabaena* and maize have been determined by X-ray crystallography (*9*, *10*), confirming the importance of the nature of the interactions that was established by biochemical studies. Thus, biochemical and structural data indicate that Fd binds in a concave cavity around the FAD group of the reductase, where residues Lys75, Leu76, and Leu78 on the FNR surface play a crucial role in complex formation, by interacting with the side chains of Glu94 and Phe65 on Fd (*5*−*9*, *11*−*14*).

Flavodoxins (Fld) are small $\alpha/\beta$ flavoproteins that contain a noncovalently bound FMN cofactor. In cyanobacteria and certain algae, Fld is synthesized instead of Fd when the organism is grown under low-iron conditions and replaces it in the transfer of one electron from PSI to FNR by shuttling between the semiquinone and hydroquinone states (*15*). Although the three-dimensional structure of *Anabaena* Fld is known (*16*), the structure of the FNR−Fld complex remains undetermined. Biochemical studies indicate that Fd and Fld interact with the same region on the FNR surface (*5*, *17*, *18*). Thus, Lys75, Leu76, and Leu78 in FNR are also essential in the stabilization of an optimal complex for ET between FNR and Fld (*7*, *17*−*19*). However, although the

† This work has been supported by Comisión Interministerial de Ciencia y Tecnología (Grant BQU2001-2520 to M.M., Grant BIO2003-00627 to C.G.-M., and Grant BMC2003-00458 to M.A.R.), the European Union (Network HPRN-CT1999-00095 to M.A.R.), and the Andalusian Government (PAI, Grant CVI-0198 to M.A.R.).

* To whom correspondence should be addressed: Departamento de Bioquímica y Biología Molecular y Celular, Facultad de Ciencias, Universidad de Zaragoza, 50009 Zaragoza, Spain. Phone: 34976762476. Fax: 34976762123. E-mail: mmedina@unizar.es.

‡ Universidad de Zaragoza.

§ Universidad de Sevilla-CSIC.

[1] Abbreviations: Cytc, Cytc$_{ox}$, and Cytc$_{rd}$, horse heart cytochrome *c* and its oxidized and reduced states, respectively; ET, electron transfer; Fld, Fld$_{ox}$, Fld$_{sq}$, and Fld$_{rd}$, flavodoxin and its oxidized, semiquinone, and reduced states, respectively; FNR, FNR$_{ox}$, FNR$_{sq}$, and FNR$_{rd}$, ferredoxin-NADP$^+$ reductase and its oxidized, semiquinone, and reduced states, respectively; $K_d$, dissociation constant; $K_a$, association constant; $k_{ap}$, apparent rate constant; $k_{et}$, electron transfer first-order rate constant; $k_{obs}$, pseudo-first-order observed rate constant; PSI, PSI$_{ox}$, and PSI$_{rd}$, photosystem I and its oxidized and reduced states, respectively; WT, wild-type.

10.1021/bi048324d CCC: $30.25 
Published on Web 12/04/2004

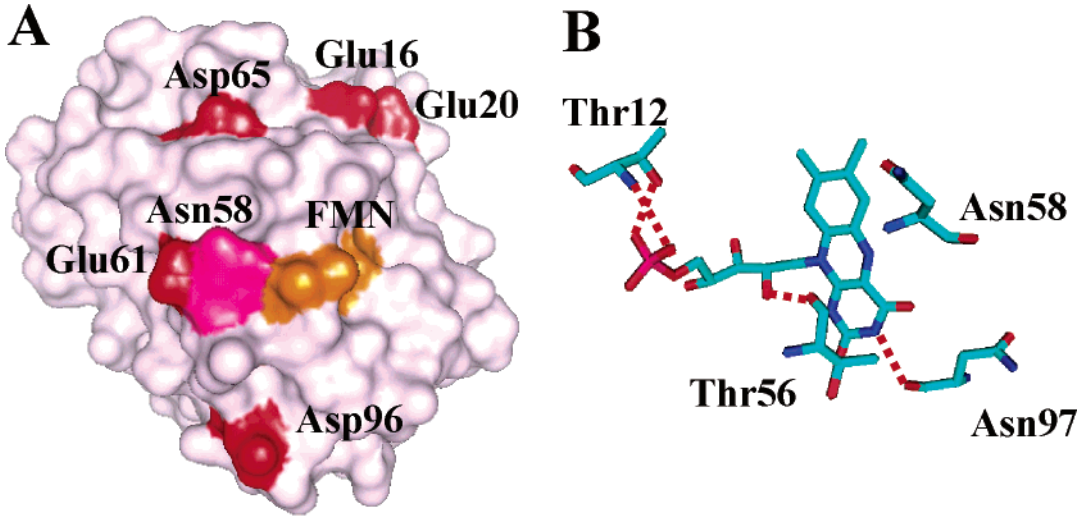


FIGURE 1: (A) Surface representation of *Anabaena* Fld showing the localization of negatively charged residues (red) Glu16, Glu20, Glu61, Asp65, and Asp96 and polar residue Asn58 (magenta). The FMN-exposed surface is colored yellow. (B) Relative position of Thr12, Thr56, Asn58, and Asn97 with respect to the FMN molecule in *Anabaena* Fld. H-Bonds are shown as red dashed lines. This figure was produced using PyMOL (*39*).

roles of several Fld residues, either acidic or hydrophobic in nature (namely, Trp57, Ile59, Glu61, Glu67, Ile92, Tyr94, Asp100, Asp126, Asp144, and Glu145), have been analyzed, none of them has shown to be critical neither for complex formation nor for ET between Fld and FNR (*19*−*22*). Thus, the two aromatic residues, Trp57 and Tyr94, that sandwich the FMN cofactor do not play an active role in the Fld redox reactions with FNR. However, these residues have been shown to be involved in setting an appropriate structural and electronic environment that modulates *in vivo* ET from PSI to FNR while also providing tight FMN binding (*22*). In addition, although the side chains of Ile59 and Ile92 Fld do not seem to be critical in the interaction and ET processes with FNR, they are important both in complex formation and in ET between PSI and Fld (*19*).

In this study, the parameters that regulate ET from PSI to FNR via Fld have been further studied by analyzing other Fld side chains that might be critical in the processes of interaction and ET with both Fld substrates, either by being involved in the protein−protein interaction or by modulating the properties of the FMN ring. We have tried to find the counterpart residue of Lys75 on the FNR surface by eliminating negatively charged side chains on the Fld surface. The following mutants have been constructed: Glu16Gln, Glu20Lys, Glu61Ala, Glu61Lys, Asp65Lys, and Asp96Asn (Figure 1A). In addition, the effect produced by replacement of Fld residues situated in the vicinity of FMN on the ET from PSI to FNR has also been analyzed by the study of the Thr12Val, Thr56Gly, Thr56Ser, Asn58Cys, Asn58Lys, and Asn97Lys Fld mutants (Figure 1B). A role has been demonstrated for some of these positions in the modulation of FMN reduction properties or/and in FMN binding to Fld (*23*, *24*).

## MATERIALS AND METHODS

*Biological Material.* Site-directed mutagenesis to produce Thr12Val, Glu16Gln, Glu20Lys, Thr56Gly, Thr56Ser, Asn58Lys, Asn58Cys, Glu61Ala, Asp65Lys, Asp96Asn, and Asn97Lys *Anabaena* sp. PCC 7119 Fld mutants was described previously (*23*−*26*). Fld mutants were overproduced in *Escherichia coli* and purified as previously described (*22*, *24*). Recombinant WT FNR was purified from *E. coli* cultures containing the FNR gene from *Anabaena* sp. PCC 7119, as previously described (*27*). UV−vis spectra and SDS−PAGE were used as purity criteria. PSI particles from *Anabaena* sp. PCC 7119 were obtained by $\beta$-dodecyl maltoside solubilization (*28*). The P700 content in PSI samples was calculated from the photoinduced absorbance changes at 820 nm using an absorption coefficient of 6.5 $mM^{-1}$ $cm^{-1}$ (*29*). The chlorophyll concentration was determined according to the method of Arnon (*30*). The chlorophyll/P700 ratio of the resulting PSI preparations was 140/1. The same batches of PSI and flavoproteins were used throughout this study.

*Spectral Analysis.* UV−vis spectra were recorded on a Kontron Uvikon 942 spectrophotometer. Dissociation constants and changes in extinction coefficients for the complexes between WT $FNR_{ox}$ and $Fld_{ox}$ were obtained by difference spectroscopy as previously described (*19*, *27*). The cuvettes contained approximately 20 $\mu$M FNR, to which aliquots of Fld were added. Dissociation constants and difference extinction coefficients for the complexes were obtained by using nonlinear regression to fit the experimental data to the theoretical equation for a 1/1 stoichiometric complex. Errors in the estimated $K_d$ and $\Delta\epsilon$ values were ±15%. Unless otherwise stated, all measurements were carried out at 25 °C in 50 mM Tris-HCl buffer (pH 8.0). CD spectra were recorded in a Jasco 710 spectropolarimeter using a cuvette with a path length of 1 cm that contained 5 mM Tris-HCl buffer (pH 8.0). The protein concentration was 0.7 $\mu$M for far-UV spectra and 4 $\mu$M for the UV−visible spectra.

*Steady-State Kinetic Analysis.* The FNR-dependent NADPH-cytochrome *c* reductase activity was assayed by using Fld as the carrier of electrons from FNR to cytochrome *c* (Cytc) (*19*, *27*), according to the following scheme:

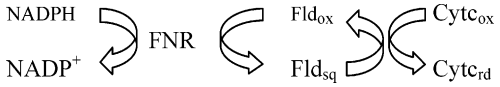

The standard reaction mixture contained, at 25 ± 1 °C, 50 $\mu$M NADPH, 2.5 nM FNR, 0.75 mM Cytc (Sigma), 50 mM Tris-HCl (pH 8.0), and different concentrations of a Fld mutant. Values for $K_m$ and $k_{cat}$ were determined by fitting the kinetic data to the Michaelis−Menten equation, and were estimated to have errors of ±15 and ±10%, respectively.

*Fast Kinetic Analysis.* Fast ET reactions between FNR and Fld and between Fld and Cytc were studied by stopped-flow spectrophotometry under anaerobic conditions in an Applied Photophysics SX17.MV spectrophotometer interfaced with an Acorn 5000 computer, using the SX.18MV software of Applied Photophysics as previously described (*19*, *27*). The apparent rate constants ($k_{ap}$) were calculated by fitting the data to mono- or biexponential processes. At least 8−10 apparent constants were averaged to calculate each final rate constant. Samples for stopped-flow analysis were made anaerobic in specially designed tonometers by several cycles of evacuation and flushing with $O_2$-free argon. Reduced FNR and Fld were prepared by photoreduction with 5-deazariboflavin (*27*). Reactions between FNR and Fld and between Fld and Cytc were followed at 600 and 550 nm, respectively, by mixing at a 1/1 molar ratio to give final protein concentrations of 10−12 $\mu$M. Reactions between Fld and Cytc were also carried out using a 1.3 molar ratio, with final Fld concentrations of 10−12 $\mu$M. Errors in the estimated $k_{ap}$ values were ±15%. All reactions were carried out in 50 mM Tris-HCl buffer (pH 8.0) at 13 °C.

The interaction and ET between PSI and Fld were analyzed by laser flash spectroscopy following absorbance changes at 580 nm at room temperature and under aerobic conditions as previously described (*19*, *22*). The wavelength of 580 nm was chosen for monitoring Fld semiquinone formation with the smallest possible contribution of PSI to the absorbance change. All the experiments were carried out in a cuvette with a path length of 1 cm at 22 ± 1 °C. Unless otherwise stated, the standard reaction mixture contained, in a final volume of 1 mL, 20 mM Tricine-KOH (pH 7.5), 0.03% $\beta$-dodecyl maltoside, an amount of PSI-enriched particles equivalent to 35 $\mu$g of chlorophyll/mL, 0.1 $\mu$M phenazine methosulfate, 2 mM magnesium chloride, 2 mM sodium ascorbate, and Fld at the indicated concentration. The ascorbate and phenazine methosulfate ensure that $PSI_{ox}$ is totally re-reduced between flashes. Data collection and analysis were as previously described (*31*, *32*). Each kinetic trace was the average of 40−50 independent measurements with a 30 s spacing between flashes. Samples were protected from actinic light between flashes by an electronic shutter synchronized with the laser trigger. The estimated error in the observed rate constants ($k_{obs}$) was less than 20%.

*In Silico Mutation and Calculation of the Surface Electrostatic Potential and Dipole Moment.* On the basis of the *Anabaena* Fld three-dimensional structure (Protein Data Bank entry 1flv), models for the different mutants have been generated using Swiss-PdbViewer (GlaxoSmithKline Research and Development). The surface electrostatic potential was calculated for each Fld variant model with version 3.7 of Swiss-PdbViewer using the Poison−Boltzman electrostatic potential tool (*33*). The dipole moment ($\mu$) for WT and mutated Flds has been calculated by using the equation $\mu = \sum q_i r_i$, $q_i$ and $r_i$ being the partial charge and the coordinates for the position, respectively, of each protein atom. The partial charge on each protein atom was taken from the AMBER force field (*34*) and that for each atom of the FMN cofactor from ref *35*. The center of mass of each protein was used as a reference position for the calculation of $\mu$.

Table 1: NADPH-Dependent Cytochrome *c* Reductase Activity of Wild-Type FNR with Different Mutated Flavodoxins as the Mediator[a]

| Fld form | $k_{cat}^{Fld}$ ($s^{-1}$) | $K_m^{Fld}$ ($\mu$M) | $k_{cat}/K_m^{Fld}$ ($\mu M^{-1}$ $s^{-1}$) |
|---|---|---|---|
| WT[b] | 23.3 | 33.0 | 0.70 |
| T12V | 11.0 | 11.1 | 1.00 |
| E16Q | 15.0 | 94.0 | 0.16 |
| E20K | 25.0 | 172.0 | 0.14 |
| T56G | 58.6 | 95.0 | 0.20 |
| T56S | 19.0 | 94.0 | 0.16 |
| N58C | nd[c] | nd[c] | nd[c] |
| N58K | 14.0 | 50.0 | 0.28 |
| E61A | 19.3 | 144.6 | 0.13 |
| E61K | 31.3 | 166.3 | 0.19 |
| D65K | 15.1 | 20.0 | 0.75 |
| D96N | 11.0 | 11.1 | 0.99 |
| N97K | 14.5 | 48.0 | 0.30 |

[a] Data obtained in 50 mM Tris-HCl (pH 8.0) at 25 °C. [b] Data from ref *27*. [c] No reaction was observed.

## RESULTS

*Expression, Purification, and Spectral Properties of the Different Fld Mutants.* The level of expression of mutants of Fld at residues Thr12, Glu16, Glu20, Thr56, Asn58, Glu61, Asp65, Asp96, and Asn97 were similar to that of the WT protein. The spectral properties (UV−vis absorption and CD spectra) of most of the mutants were also similar to those of WT Fld (see refs *23*−*26*). The shapes of the UV−vis absorption spectra and the extinction coefficients at the maxima of Thr56Gly and Asn58Lys Fld were slightly different from those of WT Fld (not shown; see ref *23*), indicating that a slight modification of the flavin ring environment had occurred. However, the CD spectra indicated that no major structural perturbations had been produced by any of the mutations.

*Steady-State Kinetic Analysis of the Different Fld Mutants.* The $k_{cat}$ values obtained for FNR when using the different Fld mutants as electron carriers in the Fld-mediated NADPH-dependent cytochrome *c* reductase assay were similar to that reported when using WT Fld. The only exception was the Thr56Gly mutant for which $k_{cat}$ was more than twice that of WT (Table 1). The mutations had stronger effects on the $K_m$. The FNR $K_m$ values for Thr12Val, Asp65Lys, and Asp96Asn Fld mutants were slightly up to 3 times lower than that for WT Fld. In contrast, the $K_m$ values for the remaining Fld mutants were greater than that of WT Fld, suggesting a loss of specificity in the interaction had occurred. The $K_m$ values for Glu16Gln, Thr56Gly, Thr56Ser, Asn58Lys, and Asn97Lys Fld were up to 3 times higher than that of WT Fld, and even weaker interactions were observed for Glu20Lys, Glu61Ala, and Glu61Lys Flds, with values up to 5-fold higher than that for WT Fld (Table 1). With three exceptions, the catalytic efficiencies ($k_{cat}/K_m$) of FNR with the different Fld variants as electron carriers were much lower than when WT Fld was used as the carrier. The exceptions were Thr12Val, Asp65Lys, and Asp96Asn Fld which had efficiencies similar to that of WT Fld. The largest effect was seen with Asn58Cys Fld, the activity of which

Table 2: Dissociation Constants and $\Delta\epsilon_{462}$ for Complex Formation of Oxidized WT FNR with WT and Mutated Flavodoxin Forms[a]

| Fld form | $K_d$ ($\mu$M) | $\Delta\epsilon_{462}$ ($mM^{-1}\,cm^{-1}$) |
|---|---|---|
| WT[b] | 3.0 | 1.4 |
| T12V | 2.2 | 1.4 |
| E16Q | 20.8 | 3.0 |
| E20K | 14.5 | 2.4 |
| T56G | 23.4 | 2.6 |
| T56S | 15.0 | 2.5 |
| N58C | 20.7 | 2.3 |
| N58K | 30.0 | 3.0 |
| E61A | 15.0 | 2.0 |
| E61K | 11.4 | 2.9 |
| D65K | 5.9 | 0.9 |
| D96N | 19.4 | 3.0 |
| N97K | 8.0 | 1.7 |

[a] Data obtained in 50 mM Tris-HCl (pH 8.0) at 25 °C. [b] Data from ref *27*.

was so low that values for $k_{cat}$ and $K_m$ could not be determined.

*Interaction of $Fld_{ox}$ Variants with WT $FNR_{ox}$.* The difference spectrum that occurs when WT $Fld_{ox}$ and $FNR_{ox}$ form a complex shows absorption maxima around 390 and 464 nm. It has been proposed that the difference spectrum arises from an alteration in the flavin environment of FNR (*22*, *27*). Similar spectral perturbations were observed for the complexes between $FNR_{ox}$ and all the $Fld_{ox}$ mutants analyzed here (not shown), indicating that the FNR flavin environment is altered to the same extent. The $K_d$ values for the complexes with Thr12Val, Asp65Lys, and Asn97Lys Fld are close to that of the complex with WT Fld, but the values determined for the rest of the mutants were greater (Table 2). Thus, the complexes with Glu20Lys, Thr56Ser, Glu61Ala, and Glu61Lys $Fld_{ox}$ forms were 4−6 times weaker than that with WT Fld, and even weaker complexes were formed with Glu16Gln, Thr56Gly, Asn58Cys, Asn58Lys, and Asp96Asn Flds ($K_d$ values up to 10 times higher). The difference extinction coefficients at 462 nm for the complexes ($\Delta\epsilon$) were all within a factor of 2.5 of that obtained with the WT protein (Table 2).

*Kinetic Analysis of the Electron Transfer between FNR and Fld Mutants.* Reduction of $FNR_{ox}$ by $Fld_{rd}$ can be followed by measuring the increase in the absorbance at 600 nm due to the formation of the flavin semiquinones of both proteins (*19*, *22*, *27*). The reaction with the WT proteins is too fast to be measured by stopped-flow spectrophotometry. However, the reaction of $FNR_{ox}$ with excess $Fld_{rd}$ is slower when mutants of FNR or Fld are used, and earlier analyses showed that the overall process takes place in two steps: formation of the semiquinones of both proteins followed by further reduction of $FNR_{sq}$ to the fully reduced state (*19*, *22*, *27*). Table 3 gives the kinetic parameters corresponding to these two processes as determined by stopped-flow. The reduction of $FNR_{ox}$ by the fully reduced forms of Thr12Val, Glu16Gln, Glu20Lys, Thr56Ser, Asp65Lys, or Asp96Asn $Fld_{rd}$ was similar to the reaction observed with WT Fld, the first process taking place mainly within the instrumental dead time ($k_{ap1} > 600\ s^{-1}$). In the reaction with the WT proteins, the second process is too fast to be distinguished from the first, and therefore, $k_{ap2}$ cannot be separated from $k_{ap1}$ (*27*). However, this process is considerably slower for some of these mutants, allowing $k_{ap2}$ to be determined (Table 3). This

Table 3: Kinetic Parameters for the Reactions of WT FNR with WT and Mutated Flavodoxin Forms[a]

| | mixing of $FNR_{ox}$ with $Fld_{rd}$ | | mixing of $FNR_{rd}$ with $Fld_{ox}$ | |
|---|---|---|---|---|
| Fld form | $k_{ap1}$ ($s^{-1}$) | $k_{ap2}$ ($s^{-1}$) | $k_{ap1}$ ($s^{-1}$) | $k_{ap2}$ ($s^{-1}$) |
| WT[b] | >600[c] | nd[c] | 2.5 | 1.0 |
| T12V | >600[c] | 45.0 | 1.0 | 0.5 |
| E16Q | >600[c] | 88.0 | 1.2 | 0.3 |
| E20K | >600[c] | 245.0 | 15.5 | 1.3 |
| T56G | nd[d] | | 25.3 | |
| T56S | >600[c] | 213.0 | 2.5 | 0.7 |
| N58C | >300[e] | 15.0 | 0.7 | 0.4 |
| N58K | >300[e] | 17.7 | 11.0 | 0.4 |
| E61A | 70.0 | 2.2 | 19.0 | 0.6 |
| E61K | 82.0 | 3.3 | 5.5 | 0.9 |
| D65K | >600[c] | nd[c] | 3.4 | 0.6 |
| D96N | >600[c] | 230.0 | 3.0 | 0.8 |
| N97K | 160 | 12.2 | 3.5 | 1.1 |

[a] Data obtained in 50 mM Tris-HCl (pH 8.0) at 25 °C. Reaction followed at 600 nm. [b] Data from ref *27*. [c] Most of the reaction occurred within the dead time of the instrument. [d] No reaction was observed. [e] Only part of the initial reaction occurred within the dead time of the instrument.

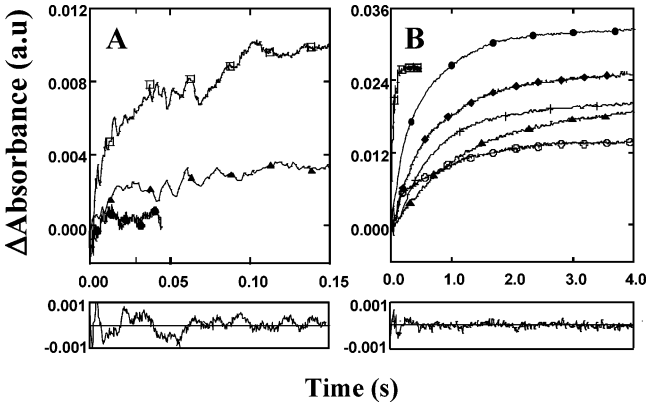


FIGURE 2: Time course for the anaerobic reactions between WT FNR and selected Fld mutants as measured by stopped-flow spectrophotometry. (A) Reaction of WT $FNR_{ox}$ with Asn58Cys $Fld_{rd}$ (●), Asn58Lys $Fld_{rd}$ (▲), and Asn97Lys $Fld_{rd}$ (□, residual for this fitting is shown at the bottom). (B) Reaction of WT $FNR_{rd}$ with WT $Fld_{ox}$ (+), Thr56Gly $Fld_{ox}$ (□), Thr56Ser $Fld_{ox}$ (◆, residual for this fitting is shown at the bottom), Asn58Cys $Fld_{ox}$ (▲), Asn58Lys $Fld_{ox}$ (○), and Glu61Lys $Fld_{ox}$ (●).

was the case for the reactions with Asn58Cys, Asn58Lys, Glu61Ala, Glu61Lys, and Asn97Lys $Fld_{rd}$ which were considerably slower than that of WT, and thus, $k_{ap}$ values for both processes can be determined (Figure 2A and Table 3). No reaction at all was observed with Thr56Gly $Fld_{rd}$.

The reverse reaction of WT $FNR_{rd}$ with WT $Fld_{ox}$ is a relatively slow two-step process. The two steps are production of both flavoprotein semiquinones ($Fld_{sq}$ and $FNR_{sq}$) followed by the reduction of a second $Fld_{ox}$ molecule by the $FNR_{sq}$ produced in the first step (given as result a second molecule of $Fld_{sq}$ and $FNR_{ox}$) (*27*). With one exception, the corresponding kinetic traces for the reaction of all $Fld_{ox}$ mutants were also best fitted to a biphasic process (Figure 2B). The exception was the Thr56Gly Fld mutant for which the kinetic trace fitted to a single-exponential process. The two $k_{ap}$ values for most of the mutants were within a factor of 2 of those of WT $Fld_{ox}$. However, the reactions with Glu20Lys, Asn58Lys, Glu61Ala, and, in particular, Thr56Gly Flds were faster (Table 3). The amplitudes of the kinetic traces for the reactions were in general within a factor of 2

Table 4: Kinetic Parameters for the Reduction of WT Cytc by WT and Mutated Fld Forms[a]

| | mixing of equimolecular amounts of $Cytc_{ox}$ with $Fld_{rd}$ | |
|---|---|---|
| Fld form | $k_{ap1}$ ($s^{-1}$) | $k_{ap2}$ ($s^{-1}$) |
| WT | 3.8 | 0.20 |
| E20K | 3.5 | 0.26 |
| T56G | 11.3 | 0.86 |
| T56S | 0.4 | 0.10 |
| E61A | 3.4 | 0.26 |
| N97K | 0.5 | 0.08 |

[a] Data obtained in 50 mM Tris-HCl (pH 8.0) at 25 °C.

of that of the WT Fld process. The only exception was observed in the Asp65Lys $Fld_{ox}$ for which the amplitude was only 25% of that observed in the corresponding reaction with WT, suggesting that in this later case the reaction is taking place to a much lesser extent. Finally, the monoexponential behavior of the process with Thr56Gly Fld, with a $k_{ap}$ value 10-fold higher than that observed for WT Fld, indicates that removal of the Thr56 side chain produces an important change in the mechanism of ET from FNR to Fld. The monoexponential behavior observed for this mutant might be due either to an almost full consumption of $FNR_{rd}$ by the first step or to a change in the mechanism of ET from the reduced FAD to the Fld FMN.

*Kinetic Analysis of Cytc Reduction by Fld Mutants.* The reaction between $Fld_{rd}$ forms and $Cytc_{ox}$ was investigated by stopped-flow methodology in an effort to determine whether the changes observed in the catalytic assay of NADPH-cytochrome *c* reductase activity might be due to alterations in the interaction and ET between Fld and Cytc. When WT $Fld_{rd}$ was reacted with $Cytc_{ox}$, an increase in absorbance at 550 nm was observed, due to $Cytc_{ox}$ reduction, and the change was best fit by a two-exponential process. This biphasic behavior has been proposed to be consistent with the production of $Cytc_{rd}$ and $Fld_{sq}$ and then reduction of a second $Cytc_{ox}$ molecule by $Fld_{sq}$ (*19*). Similar two-exponential kinetics were observed for selected Fld mutants (Table 4), but the values for the apparent rate constants were different from those determined with WT Fld. The rate constants determined from the reaction of $Cytc_{ox}$ with Glu20Lys and Glu61Ala $Fld_{rd}$ were similar to those determined with WT $Fld_{rd}$, indicating that Glu20 and Glu21 do not play a role in the Cytc−Fld interaction. In contrast, the rate constants determined for Thr56Gly $Fld_{rd}$ were 4-fold greater, while for Thr56Ser and Asn97Lys $Fld_{rd}$, they are smaller, indicating that these mutants are less efficient in the process of ET to $Cytc_{ox}$ (Table 4). It is notable that while for most of the mutants the $k_{ap}$ values increased with an increase in the concentration of Cytc, the $k_{ap}$ values for the reduction of $Cytc_{ox}$ by Thr56Gly $Fld_{rd}$ decreased with an increase in Cytc concentration (not shown).

*Kinetic Analysis of Reduction of Fld Mutants by PSI.* To gain deeper insight into the interaction forces and ET features involved in the reduction of Fld by $PSI_{rd}$, we also analyzed the reactivity of the different *Anabaena* $Fld_{ox}$ mutants toward PSI using laser flash absorption spectroscopy. Reduction of Fld mutants to the semiquinone state by $PSI_{rd}$ followed monoexponential kinetics for WT and all of the mutants (not shown). The pseudo-first-order rate constants ($k_{obs}$) for reduction of WT, Thr12Val, Glu16Gln, Thr56Gly, and

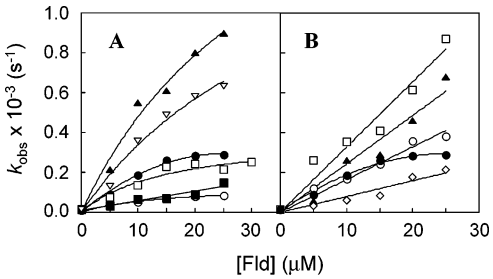


FIGURE 3: Dependence of the $k_{obs}$ for reduction of Fld by PSI on Fld concentration. (A) WT (●), Thr12Val (○), Glu16Gln (□), Thr56Gly (▲), Asn58Lys (■), and Asn97Lys (▽). (B) WT Fld (●), Thr56Ser (○), Glu61Ala (▲), Glu61Lys (□), and Asp96Asn (◇).

Table 5: Kinetic Parameters for the Reduction of WT and Mutated Flavodoxin Forms by PSI[a]

| Fld form | $K_a$ (M) | $k_{et}$ ($s^{-1}$) | $k_2$ ($M^{-1}\,s^{-1}$) |
|---|---|---|---|
| WT | $2.0 \times 10^5$ | 490 | |
| T12V | $1.0 \times 10^5$ | 130 | |
| E16Q | $1.5 \times 10^5$ | 350 | |
| E20K | *b* | *b* | $2.9 \times 10^6$ |
| T56G | $0.8 \times 10^5$ | 1500 | |
| T56S | *b* | *b* | $1.5 \times 10^7$ |
| N58C | *b* | *b* | $5.1 \times 10^6$ |
| N58K | *b* | *b* | $4.8 \times 10^6$ |
| E61A | *b* | *b* | $2.4 \times 10^7$ |
| E61K | *b* | *b* | $2.6 \times 10^7$ |
| D65K | *b* | *b* | $8.4 \times 10^6$ |
| D96N | *b* | *b* | $7.1 \times 10^6$ |
| N97K | $1.0 \times 10^5$ | 1500 | |

[a] Data obtained in 20 mM Tricine-KOH (pH 7.5) at 22 °C. [b] The dependence of $k_{obs}$ on Fld concentration was linear.

Asn97Lys Flds by PSI were found to depend nonlinearly on the Fld concentration, showing a saturation profile (Figure 3A), as previously reported for the WT *Anabaena* Fld−PSI system (*19*, *20*, *22*, *36*). This suggests that a bimolecular transient $PSI_{rd}$−$Fld_{ox}$ complex is formed prior to ET, according to a minimal two-step reaction mechanism described previously (*20*, *37*, *38*), and allows the ET first-order rate constant ($k_{et}$) to be estimated (experimentally inferred from the limiting $k_{obs}$ at an infinite Fld concentration) together with the equilibrium constant for complex formation ($K_a$) (*32*). The values obtained for $K_a$ and $k_{et}$ are shown in Table 5. Replacing either Thr56 with Gly or Asn97 with Lys caused a 3-fold increase in the $k_{et}$ value and a 2-fold decrease in the $K_a$ value compared to those of WT Fld, whereas the Glu16Gln Fld mutant behaved like WT Fld. The efficiency of the reduction of the Thr12Val mutant by PSI was, in its turn, significantly poorer compared with the WT system, showing both lower $k_{et}$ and $K_a$ values (Table 5).

The remaining Fld mutants exhibited a linear dependence of $k_{obs}$ on Fld concentration (Figure 3). This indicates that $PSI_{rd}$ and these $Fld_{ox}$ mutants react by means of a collisional-type mechanism, in which no detectable transient complex is formed. Second-order bimolecular rate constants ($k_2$) for Fld reduction can be estimated from the linear plots shown in Figure 3 (Table 5). It is interesting to note that although the observed linear dependences indicated that the equilibrium constant for complex formation was decreased, the $k_{obs}$ values obtained at high Fld concentrations for the Glu61Ala and Glu61Lys Fld mutants are higher than for WT Fld (Figure 3B). In contrast, the Asn58Cys and Asn58Lys Fld mutants gave $k_{obs}$ values that are 3-fold smaller, while the

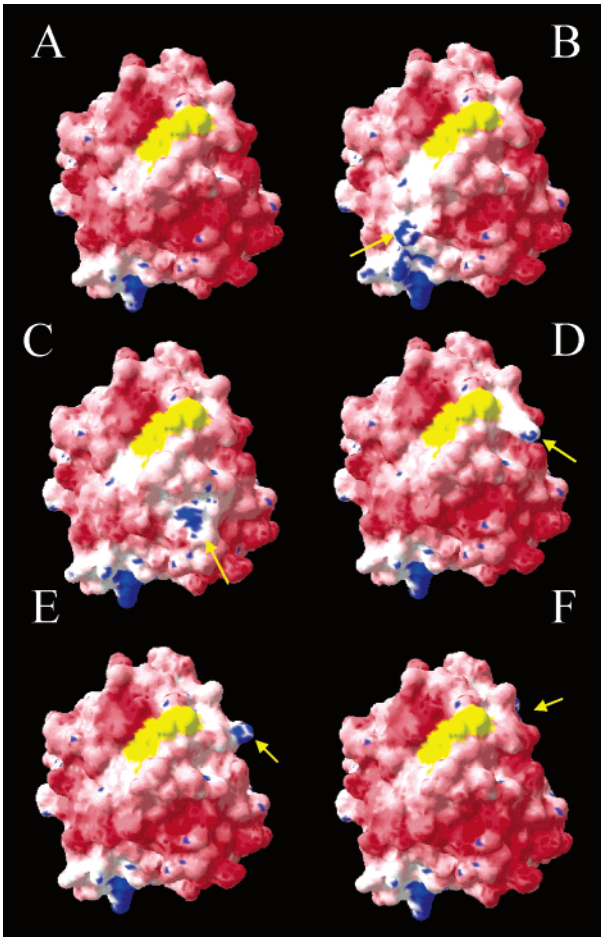


FIGURE 4: Molecular surface representation of Fld showing the electrostatic potential. Negative potential is represented in red and positive potential in blue. The exposed surface of the FAD cofactor is colored yellow: (A) WT Fld, (B) Glu20Lys, (C) Asp65Lys, (D) Asn58Lys, (E) Glu61Lys, and (F) Asn97Lys. Arrows show the localization of the mutation on the protein surface. This figure was produced using the Poisson−Boltzmann electrostatic potential tool as implemented in Swiss-PdbViewer 3.7 (*33*).

values for the Glu20Lys, Thr56Ser, Asp65Lys, and Asp96Asn mutants were similar to those of WT Fld (Figure 3 and Table 5).

## DISCUSSION

Surface electrostatic potential and dipole moment calculations indicate that there is very strong dipole in the Fld molecule (Table 6 and Figure 4A). The N-terminal residues are the only ones that produce an accumulation of positive potential on the surface (Figure 4A), pointing the negative dipole of the molecule toward the flavin ring. Several charged residues on the surface of Fld and in the FMN environment have been replaced (namely, Glu16, Glu20, Glu61, Asp65, and Asp96) (Figure 1A). With the exception of Asp65, the Fld mutants exhibit a slight weakening of the interaction or a decrease in the rate of the ET processes with FNR (Tables 1 and 2). The mutations introduced at Asp61 side chains are the ones that most impair complex formation and ET. Since the reduction potentials for these mutants are similar to those of WT Fld (*23*), the observed effects have to be the result of slightly different modes of interaction of Fld with FNR. Analysis of the surface electrostatic potentials of the mutants indicates that the mutations produce very localized effects by including small and localized patches of positive

Table 6: Dipole Moments for WT and Mutated Flavodoxin Forms

| Fld form | dipole moment (D) | deviation with regard to the orientation of the WT dipole moment (deg) |
|---|---|---|
| WT | 699 | 0.0 |
| T12V | 701 | 0.0 |
| E16Q | 666 | 5.23 |
| E20K | 669 | 12.68 |
| T56G | 702 | 0.18 |
| T56S | 700 | 0.03 |
| N58C | 700 | 0.28 |
| N58K | 607 | 2.71 |
| E61A | 631 | 3.66 |
| E61K | 557 | 9.77 |
| D65K | 593 | 9.96 |
| D96N | 636 | 7.03 |
| N97K | 644 | 6.18 |

electrostatic potential (Figure 4B,C,E). The data suggest that none of these mutations breaks single salt bridges that are crucial for the interaction and, therefore, that none of these Fld side chains resembles the critical role played by Glu94 on Fd (*12*). Nevertheless, our data indicate that residues Glu16, Glu20, Asp65, Asp96, and, in particular, Glu61 contribute to the correct FNR−Fld interaction for efficient ET (Tables 1−3). The dipole moment of the mutants compared with that of WT Fld suggests that the observed effects might be related to alterations in the module and direction of the overall dipole of Fld (Table 6). Such changes might produce orientations between Fld and FNR that are weak or nonoptimal for ET, or even others that are more adequate for ET. Superposition of the X-ray structure coordinates of FNR and Fld onto those for NADPH-cytochrome P450 reductase, an enzyme that comprises FNR and Fld domains, might provide a good model for the FNR−Fld interaction. This model leads to a shortest distance between the two flavin rings of ∼4 Å and suggests that Fld could be oriented in different ways on the FNR surface without significantly altering the distance between the methyl groups of FAD and FMN (*7*). If the main requirement for ET is the proximity of the redox centers in a nonpolar environment, this might explain why mutagenesis of the individual residues has not revealed one that is critical for the efficient interaction with FNR and why subtle changes in the Fld surface electrostatic potential and dipole moment still produce complexes that allow ET.

The roles in FNR−Fld interaction and ET of residues located close to the FMN of Fld have also been analyzed (Figure 1B). No major alterations were observed in the parameters of the Thr12Val Fld reactions, indicating that the side chain of Thr12 is not involved in either association or ET, but rather has a role in FMN binding (*24*). Mutations introduced at residues Thr56, Asn58, and Asn97 produced slightly weaker interactions with FNR (Tables 1 and 2), mainly altering the ET process (Tables 1 and 3). Replacement of Thr56 with Gly enhances ET from $FNR_{rd}$ to $Fld_{ox}$ (Tables 1 and 3), whereas the reverse ET reaction from $Fld_{rd}$ to $FNR_{ox}$ (Table 3) was abolished. This mutation increases $E_{sq/rd}$ by 63 mV (to −376 mV), whereas the corresponding replacement by Ser has no effect on the reduction potential (*23*). The $E_{sq/rd}$ value for the Thr56Gly mutant suggests that full reduction by $FNR_{rd}$ ($E_{ox/rd} = -374$ mV) might be achieved. However, analysis of the reaction by stopped-flow spectrophotometry indicates that the semiquinones of both proteins

accumulate, an observation that is not consistent with a two-electron transfer process. Since $E_{ox/sq}$ for this mutant is similar to that of WT Fld, structural aspects that affect the flavin environment must account for the observed effect. A similar behavior has been reported for replacement of Tyr94 with Ala (*22*), the authors concluding that enhancement of ET from $FNR_{rd}$ to $Fld_{ox}$ was due to the greater accessibility of the isoalloxazine of FMN. In support of this, the theoretical three-dimensional structure for Thr56Gly Fld (see Figure 8 from ref *23*) suggests that the FMN in this mutant is more accessible to the solvent when Fld is free in solution and, presumably, more accessible to reduction when it is in a complex with FNR. Since no reaction at all was observed for the reverse process when the reduced form of this mutant was mixed with oxidized FNR, we cannot determine whether this reaction is not taking place at all or it is too fast to be detected. The alteration of $E_{sq/rd}$ (+63 mV) cannot explain either of the two possibilities, and accessibility of the FMN and structural factors around the flavin ring should account for it. The importance of the FMN accessibility in the ET processes is also explained by analyzing the ability of these mutants to reduce Cytc (Table 4). Thus, although the driving force for the process is large enough for the reactions with both Thr56Gly and Thr56Ser Flds, Thr56Gly Fld reduces Cytc faster than WT Fld whereas the ET process from Thr56Ser $Fld_{rd}$ is considerably hindered.

Replacement of Asn58 with Cys or Lys and of Ans97 with Lys produced Flds that donate electrons to FNR more slowly than WT Fld (Table 3). Replacement of Asn58 with Cys hindered the reverse process (Tables 1 and 3), but replacement with Lys seems to enhance the ET process itself (Table 3). The behavior of the reoxidation process of the Asn58Cys mutant cannot be explained thermodynamically, since the mutation does not lead to major changes in its reduction potential (*23*). The weaker interaction of the oxidized forms of this mutant with $FNR_{ox}$ might promote a different mutual orientation of the protein electrostatic surfaces, making the complex less optimal for ET (Figure 4D,F). Introduction of a Lys side chain at positions Asn58 or Asn97 has been shown to make $E_{sq/rd}$ less negative (32 and 18 mV, respectively) and $E_{ox/sq}$ more negative (−23 and −16 mV, respectively), which might account in some degree for the alterations in the kinetic parameters. Other explanations for the effects, such as different orientations between the redox centers in the complexes formed with FNR, due to changes in the dipole moment of these Fld mutants (Table 6), or structural aspects that affect the flavin environment, cannot be discarded.

Interaction and ET between $PSI_{rd}$ and $Fld_{ox}$ mutants were analyzed by laser flash photolysis. The results indicate that in the mutants in which negative charges had been removed, ET no longer takes place by formation of a transient complex but rather through a collisional-type mechanism, with the exception being the Glu16Gln mutant (Figure 3). The data indicate that residues Glu20, Glu61, Asp65, and Asp96 play an important role in the interaction of Fld with PSI, presumably through the formation of salt bridges. Moreover, the $k_{obs}$ values obtained for the Glu61Ala and Glu61Lys Flds are greater at all the PSI/Fld ratios assayed than those obtained for the WT protein, suggesting that the WT complex is not optimized for ET, which can be explained as the complex favoring protein−protein specificity versus kinetic efficiency.

The association constants for the $PSI_{rd}$−$Fld_{ox}$ complexes with the Thr12Val, Thr56Gly, and Asn97Lys mutants are similar to that for the complex with WT Fld, indicating that the ability of Fld to bind PSI is not affected by the mutations. However, differences are observed for $k_{et}$. The $k_{et}$ for the reaction between $PSI_{rd}$ and Thr12Val $Fld_{ox}$ is ∼4-fold lower than that for WT Fld, suggesting that the complex with the mutant protein is not optimal for ET. Since Thr12 is not accessible to the Fld surface, the observed effect has to be related to changes in the properties of the FMN. The values for $k_{et}$ for the reactions between $PSI_{rd}$ and Thr56Gly and Asn97Lys $Fld_{ox}$ mutants are increased ∼3-fold. These differences can again be due to a greater accessibility of the flavin cofactor in the Thr56Gly mutant, as was the case for the Tyr94Ala Fld mutant (*22*), or to changes in the isoalloxazine environment that influence the flavin reduction properties. Complex formation with PSI is impaired in Thr56Ser, Asn58Cys, and Asn58Lys Fld mutants. Thr56 is not accessible to the Fld surface, suggesting that in the Thr56Ser mutant the observed effect is related to changes in the FMN properties. In contrast, the side chain of Asn58 is exposed to the solvent, and the data suggest that this residue is involved in the interaction with PSI. In addition, mutations at position 58 make $k_{obs}$ at a given protein concentration smaller than the corresponding value for WT Fld. This can be the consequence of either a different structural FMN environment that affects the ET mechanism or an orientation between the protein dipoles not optimal for ET. Moreover, the more negative $E_{ox/sq}$ for the Asn58Lys mutant (−33 mV), compared to that of WT Fld (*23*), might influence its kinetic behavior by decreasing the driving force for the reduction of Fld by $PSI_{rd}$.

In conclusion, our data suggest that Glu16, Glu20, Glu61, Asp65, and Asp96 contribute to the right orientation and strengthening of the FNR−Fld or Fld−PSI complexes in attainment of an efficient ET, probably through the formation of weak salt bridges that produce a cooperative effect. However, taken together, our data indicate that the side chains of these amino acids are not involved in the formation of "crucial" salt bridges for optimal interaction with either FNR or PSI. The data also support the idea that the FNR−Fld interaction is less specific than the corresponding FNR−Fd interaction (*7*, *19*). Finally, the analysis of mutants of the FMN environment in Fld clearly indicates that the subtle modulation of the isoalloxazine environment influences not only the ability of Fld to exchange electrons but also its abilities to bind its physiological partners.

## ACKNOWLEDGMENT

We thank Jorge Estrada for development of the program for calculating dipole moments.

## REFERENCES

1. Wilson, I. A., and Stanfield, R. L. (1994) Antibody−antigen interactions: New structures and new conformational changes, *Curr. Opin. Struct. Biol. 4*, 857−867.
2. DeLano, W. L., Ultsch, M. H., de Vos, A. M., and Wells, J. A. (2000) Convergent solutions to binding at a protein−protein interface, *Science 287*, 1279−1283.
3. Hurley, J. K., Schmeits, J. L., Genzor, C., Gómez-Moreno, C., and Tollin, G. (1996) Charge reversal mutations in a conserved acidic patch in *Anabaena* ferredoxin can attenuate or enhance electron transfer to ferredoxin:$NADP^+$ reductase by altering

protein/protein orientation within the intermediate complex, *Arch. Biochem. Biophys. 333*, 243−250.
4. Hurley, J. K., Hazzard, J. T., Martínez-Júlvez, M., Medina, M., Gómez-Moreno, C., and Tollin, G. (1999) Electrostatic forces involved in orientating *Anabaena* ferredoxin during binding to *Anabaena* ferredoxin NADP$^+$ reductase: Site specific mutagenesis, fast kinetic measurements and electrostatic surface potential, *Protein Sci. 8*, 1614−1622.
5. Hurley, J. K., Morales, R., Martínez-Júlvez, M., Brodie, T. B., Medina, M., Gómez-Moreno, C., and Tollin, G. (2002) Structure−function relationships in *Anabaena* ferredoxin/ferredoxin:NADP$^+$ reductase electron transfer: Insights from site-directed mutagenesis, transient absorption spectroscopy and X-ray crystallography, *Biochim. Biophys. Acta 1554*, 5−21.
6. Martínez-Júlvez, M., Medina, M., Hurley, J. K., Hafezi, R., Brodie, T. B., Tollin, G., and Gómez-Moreno, C. (1998) Lys75 of *Anabaena* ferredoxin-NADP$^+$ reductase is a critical residue for binding ferredoxin and flavodoxin during electron transfer, *Biochemistry 37*, 13604−13613.
7. Medina, M., and Gómez-Moreno, C. (2004) Interaction of ferredoxin-NADP$^+$ reductase with its substrates: Optimal interaction for efficient electron transfer, *Photosynth. Res. 79*, 113−131.
8. Martínez-Júlvez, M., Nogués, I., Faro, M., Hurley, J. K., Brodie, T. M., Mayoral, T., Sanz-Aparicio, J., Hermoso, J. A., Stankovich, M. T., Medina, M., Tollin, G., and Gómez-Moreno, C. (2001) Role of a cluster of hydrophobic residues near the FAD cofactor in *Anabaena* PCC 7119 ferredoxin-NADP$^+$ reductase for optimal complex formation and electron transfer to ferredoxin, *J. Biol. Chem. 276*, 27498−27510.
9. Morales, R., Charon, M.-H., Kachalova, G., Serre, L., Medina, M., Gómez-Moreno, C., and Frey, M. (2000) A redox dependent interaction between two electron-transfer partners involved in photosynthesis, *EMBO Rep. 1*, 271−276.
10. Kurisu, G., Kusunoki, M., Katoh, E., Yamazaki, T., Teshima, K., Onda, Y., Kimata-Ariga, Y., and Hase, T. (2001) Structure of the electron-transfer complex between ferredoxin and ferredoxin-NADP$^+$ reductase, *Nat. Struct. Biol. 8*, 117−121.
11. Hurley, J. K., Cheng, H., Xia, B., Markley, J. L., Medina, M., Gómez-Moreno, C., and Tollin, G. (1993) An aromatic amino acid is required at position 65 in *Anabaena* ferredoxin for rapid electron transfer to ferredoxin-NADP$^+$ reductase, *J. Am. Chem. Soc. 115*, 11698−11701.
12. Hurley, J. K., Medina, M., Gómez-Moreno, C., and Tollin, G. (1994) Further characterization by site-directed mutagenesis of the protein−protein interface in the ferredoxin/ferredoxin:NADP$^+$ reductase system from *Anabaena*: Requirement of a negative charge at position 94 in ferredoxin for rapid electron transfer, *Arch. Biochem. Biophys. 312*, 480−486.
13. Jelesarov, W., De Pascalis, A. R., Koppenol, W. H., Hirasawa, M., Knaff, D. B., and Bosshard, H. R. (1993) Ferredoxin binding site on ferredoxin-NADP$^+$ reductase. Differential chemical modification of free and ferredoxin-bound enzyme, *Eur. J. Biochem. 216*, 57−66.
14. Karplus, P. A., and Bruns, C. M. (1994) Structure−function relations for ferredoxin-NADP$^+$ reductase, *J. Bioenerg. Biomembr. 26*, 89−99.
15. Rogers, L. J. (1987) Ferredoxins, flavodoxins and related proteins: Structure, function and evolution, in *The Cyanobacteria* (Fay, P., and Van Baalen, C., Eds.) pp 35−67, Elsevier, Amsterdam.
16. Rao, S. T., Shaffie, F., Yu, C., Satyshur, K. A., Stokman, B. J., Markley, J. L., and Sundarlingam, M. (1992) Structure of the oxidized long-chain flavodoxin form *Anabaena* 7120 at 2 Å resolution, *Protein Sci. 1*, 1413−1427.
17. Martínez-Júlvez, M., Hermoso, J., Hurley, J. K., Mayoral, T., Sanz-Aparicio, J., Tollin, G., Gómez-Moreno, C., and Medina, M. (1998) Role of Arg100 and Arg264 from *Anabaena* PCC7119 ferredoxin-NADP$^+$ reductase for optimal binding and electron transfer, *Biochemistry 37*, 17680−17691.
18. Martínez-Júlvez, M., Medina, M., and Gómez-Moreno, C. (1999) Ferredoxin-NADP$^+$ reductase uses the same site for the interaction with ferredoxin and flavodoxin, *J. Biol. Inorg. Chem. 4*, 568−578.
19. Nogués, I., Martínez-Júlvez, M., Navarro, J. A., Hervás, M., de la Rosa, M. A., Gómez-Moreno, C., and Medina, M. (2003) Role of hydrophobic interactions in the flavodoxin mediated electron transfer from photosystem I to ferredoxin-NADP$^+$ reductase in PCC 7119, *Biochemistry 42*, 2036−2045.
20. Navarro, J. A., Hervás, M., Genzor, C. G., Cheddar, G., Fillat, M. F., de la Rosa, M. A., Gómez-Moreno, C., Cheng, H., Xia, B., and Chae, Y. K. (1995) Site-specific mutagenesis demonstrates that the structural requirements for efficient electron transfer in *Anabaena* ferredoxin and flavodoxin are highly dependent on the reaction partner: Kinetic studies with photosystem I, ferredoxin:NADP$^+$ reductase, and cytochrome *c*, *Arch. Biochem. Biophys. 32*, 229−238.
21. Jenkins, C. M., Genzor, C. G., Fillat, M. F., Waterman, M. R., and Gómez-Moreno, C. (1997) Negatively charged *Anabaena* flavodoxin residues are important for reconstitution of cytochrome P450 17a hydroxylase activity, *J. Biol. Chem. 272*, 22509−22513.
22. Casaus, J. L., Navarro, J. A., Hervás, M., Lostao, A., de la Rosa, M. A., Gómez-Moreno, C., Sancho, J., and Medina, M. (2002) *Anabaena* sp. PCC 7119 flavodoxin as electron carrier from photosystem I to ferredoxin-NADP$^+$ reductase, *J. Biol. Chem. 277*, 22338−22344.
23. Nogués, I., Mayhew, S. G., Campos, L. A., Sancho, J., Gómez-Moreno, C., and Medina, M. (2004) Role of the close environment of FMN in *Anabaena* flavodoxin in the modulation of the flavin reduction potentials and in the energetics of the FMN:apoprotein interaction, *Biochemistry 43* (in press).
24. Lostao, A., El Harrous, M., Daoudi, F., Romero, A., Parody-Morreales, A., and Sancho, J. (2000) Dissecting the energetics of the apoflavodoxin-FMN complex, *J. Biol. Chem. 275*, 9518−9516.
25. Irún, M. P., García-Mira, M. M., Sanchez-Ruiz, J. M., and Sancho, J. (2001) Native hydrogen bonds in a molten globule of the apoflavodoxin thermal intermediate, *J. Mol. Biol. 306*, 877−888.
26. Irún, M. P., Maldonado, S., and Sancho, J. (2001) Stabilization of apoflavodoxin by replacing hydrogen bonded charged Asp or Glu residues by the neutral isosteric Asn or Gln, *Protein Eng. 14*, 173−181.
27. Medina, M., Martínez-Júlvez, M., Hurley, J. K., Tollin, G., and Gómez-Moreno, C. (1998) Involment of glutamic acid 301 in the catalytic mechanism of ferredoxin-NADP$^+$ reductase from *Anabaena* PCC 7119, *Biochemistry 37*, 2715−2728.
28. Hervás, M., Ortega, J. M., Navarro, J. A., de la Rosa, M. A., and Bottin, H. (1994) Laser flash kinetic analysis of *Synechocystis* PCC 6803 cytochrome $c_6$ and plastocyanin oxidation by photosystem I, *Biochim. Biophys. Acta 1184*, 235−241.
29. Mathis, P., and Sétif, P. (1981) Near infrared absorption spectra of the chlorophyll *a* cations and triplet states *in vitro* and *in vivo*, *Isr. J. Chem. 21*, 316−320.
30. Arnon, D. I. (1949) Copper enzymes in isolated chloroplasts. Polyphenoloxidase in $\beta$-vulgaris, *Plant Physiol. 24*, 1−15.
31. Hervás, M., Navarro, J. A., Díaz, A., Bottin, H., and de la Rosa, M. A. (1995) Laser-flash kinetic analysis of the fast electron transfer from plastocyanin and cytochrome $c_6$ to photosystem I. Experimental evidence on the evolution of the reaction mechanism, *Biochemistry 34*, 11321−11326.
32. Meyer, T. E., Zhao, Z. G., Cusanovich, M. A., and Tollin, G. (1993) Transient kinetics of electron transfer from a variety of c-type cytochromes to plastocyanin, *Biochemistry 32*, 4552−4559.
33. Guex, N., and Peitsch, M. C. (1997) SWISS-MODEL and the Swiss-PdbViewer: An environment for comparative protein modelling, *Electrophoresis 18*, 2714−2723.
34. Cornell, W. D., Cieplak, P., Bayly, C. I., Gould, I. R., Merz, K. M., Ferguson, D. M., Spellmeyer, D. C., Fox, T., Caldwell, J. W., and Kollman, P. A. (1995) A second generation force field for the simulation of proteins and nucleic acids, *J. Am. Chem. Soc. 117*, 5179−5197.
35. Schneider, C., and Suhnel, J. (1999) A molecular dynamics simulation of the flavin mononucleotide-RNA aptamer complex, *Biopolymers 50*, 287−302.
36. Sétif, P. (2001) Ferredoxin and flavodoxin reduction by photosystem I, *Biochim. Biophys. Acta 1507*, 161−179.
37. Medina, M., Hervás, M., Navarro, J. A., de la Rosa, M. A., Gómez-Moreno, C., and Tollin, G. (1992) A laser flash absorption spectroscopy study of *Anabaena* sp. PCC 7119 flavodoxin photoreduction by photosystem I particles from spinach, *FEBS Lett. 313*, 239−242.
38. Mühlenhoff, U., and Sétif, P. (1996) Laser flash absorption spectroscopy study of flavodoxin reduction by photosystem I in *Synechococcus* sp. PCC 7002, *Biochemistry 35*, 1367−1374.
39. DeLano, W. L. (2002) *The PyMOL Molecular Graphics System*, DeLano Scientific, San Carlos, CA.

BI048324D